

Article

Evaluation of the Absorption of Methionine Carried by Mineral Clays and Zeolites in Porcine *Ex Vivo* Permeability Models

Carlotta Giromini ^{1,*}, Marco Tretola ^{1,2,*}, Cinzia Cristiani ³, Elisabetta Finocchio ⁴, Paolo Silacci ², Sara Panseri ¹, Matteo Dell'Anno ¹, Antonella Baldi ¹ and Luciana Rossi ¹

¹ Dipartimento di Scienze Veterinarie per la Salute, la Produzione Animale e la Sicurezza Alimentare (VESPA), Università Degli Studi di Milano, Via dell'Università 6, 26900 Lodi, Italy; sara.panseri@unimi.it (S.P.); matteo.dellanno@unimi.it (M.D.); antonella.baldi@unimi.it (A.B.); luciana.rossi@unimi.it (L.R.)

² Federal Department of Economic Affairs, Education and Research EAER, Agroscope, La Tioleyre 4, 1725 Posieux, Switzerland; paolo.silacci@agroscope.admin.ch

³ Dipartimento di Chimica, Materiali e Ingegneria Chimica "G. Natta" CMIC, Politecnico di Milano, Piazza Leonardo da Vinci, 32, 20133 Milano, Italy; cinzia.cristiani@polimi.it

⁴ Dipartimento di Ingegneria Civile, Chimica e Ambientale, Università di Genova, 16145 Genoa, Italy; elisabetta.finocchio@unige.it

* Correspondence: carlotta.giromini@unimi.it (C.G.); marco.tretola@agroscope.admin.ch (M.T.)

† These authors contributed equally to the work.



Citation: Giromini, C.; Tretola, M.; Cristiani, C.; Finocchio, E.; Silacci, P.; Panseri, S.; Dell'Anno, M.; Baldi, A.; Rossi, L. Evaluation of the Absorption of Methionine Carried by Mineral Clays and Zeolites in Porcine *Ex Vivo* Permeability Models. *Appl. Sci.* **2021**, *11*, 6384. <https://doi.org/10.3390/app11146384>

Academic Editor: Nikolaos Koukouzas

Received: 16 June 2021

Accepted: 8 July 2021

Published: 10 July 2021

Publisher's Note: MDPI stays neutral with regard to jurisdictional claims in published maps and institutional affiliations.



Copyright: © 2021 by the authors. Licensee MDPI, Basel, Switzerland. This article is an open access article distributed under the terms and conditions of the Creative Commons Attribution (CC BY) license (<https://creativecommons.org/licenses/by/4.0/>).

Abstract: Supplemental dietary amino acids (AAs) need to be provided in a form that prevents their degradation along the gastrointestinal tract to guarantee their high bioavailability and bioactivity. In this study, methionine (Met) protected via organo-clay intercalation (natural carriers) has been developed as a sustainable alternative to polymeric coating. Specifically, two different bentonite-zeolite-based mineral clays were tested, Adsorbene (ADS) and BioKi (BIO). Briefly, 1 g of the carrier (ADS or BIO) was contacted with 50 mL of an aqueous solution at a pH of 3.0, 5.8, and 8.9. Solid-liquid separation was conducted. The released Met in the liquid phase was analysed by Chemical Oxygen Demand, while residual Met in the solid phase was analysed by Fourier Transform Infra-Red (FT-IR) spectroscopy. The effect of Met-ADS complex on cell viability was tested on IPEC-J2 cells incubated 3 h with Met-ADS 2.5 mM. Jejunum segments obtained by entire male pigs (Swiss Large White, body weight 100 ± 5 kg) were used as *ex vivo* models to compare the absorption of 2.5 mM Met released by ADS with 2.5 mM free Met and its influence on epithelial integrity in perfusion Ussing chambers. The carriers released a very low amount of Met and Met-BIO interaction was stronger than Met-ADS. The maximum release of Met was at pH 3, with 3% and 6% of Met release from Met-BIO and Met-ADS, respectively. Cell viability experiments revealed that Met-ADS did not alter cell metabolic activity. No differences in Met absorption and intestinal epithelial integrity were observed *ex vivo* between free Met and Met-ADS. This study provided new insights into the release of Met from natural clays such as ADS and BIO, the safety of its use in the porcine intestine and the ability of ADS-released Met to absorb to the same extent as the free Met in porcine jejunum.

Keywords: micronutrient; intestinal absorption; amino acids; IPEC-J2 cell; intestinal model; absorption; methionine; mineral clays; zeolites; pig

1. Introduction

In recent years, the application of low protein diets has been recognised as a tool in pig production to reduce feeding costs, nitrogen excretion and effectively improve gut health in an era of increasing antibiotic use limitations [1–3]. The swine industry has witnessed the great advantage of reducing dietary crude protein with free amino acids supplementation for sustainable production, saving protein ingredients, reducing nitrogen excretion, feed costs and the risk of gut disorders without impairing growth performance, compared with traditional diets [4].

Among essential amino acids, methionine (Met) has key importance in protein synthesis, methyl donation, and in antioxidant and immune defense processes in swine [5]. Free Met delivery may recover growth performance in pigs receiving a Met-deficient diet [6,7] due to nitrogen retention and muscle protein accretion by increasing protein biosynthesis [8] and decreasing protein degradation [9].

However, thermal processing has negative effects on sulfur amino acids such as Met and cystine. Therefore, supplemental dietary AAs need to be provided in a form preventing their degradation during technological treatments to guarantee high bioavailability in the organism.

Although the protection of amino acids finds its natural application in dairy cow feeding due to its essential role in rumen protection [10,11], the application of delivery systems may represent an efficient solution for reducing peptide-food matrix reactions and food processing protection.

An important prerequisite of a good delivery system, as applied to the encapsulation of food bioactive, is that it must not modify the physicochemical and organoleptic properties of the product [12] nor have reactivity with the nutritional compound. A broad spectrum of colloidal systems has been proposed as carriers for oral peptides delivery, such as liposomes, microemulsions, emulsions, biopolymer microgels, and solid lipid nanoparticles [13,14].

Our group developed a protocol for the protection of Met via organoclay intercalation (natural carriers) as more sustainable alternatives to polymeric coating [15,16]. In particular, two different bentonite-zeolite-based mineral clays were tested, Adsorbene (ADS) and BioKi (BIO). In the present study, the release of Met from ADS (Met-ADS) and BIO (Met-BIO) was tested. Furthermore, given the higher Met release from Met-ADS, its effect on *in vitro* culture of porcine intestinal epithelial cells (IPEC-J2) and Met absorption capacity in jejunum using an *ex vivo* porcine permeability model were tested.

2. Materials and Methods

The samples considered for this study were prepared according to [15,16], which allows for intercalation of neutral organic molecules without ions exchange [11,17].

Methionine (Met), C₅H₁₁NO₂S, (Supplied by Istituto delle Vitamine S.P.A., Segrate MI, (Italy), purity > 98.7%), were contacted with natural commercial clay, Adsorbene[®] (Biomicon S.R.L., Biomicon S.R.L., Torino TO, (Italy), ADS in the following), and BioKi[®] (Antika Officina Botanika S.R.L., Collecchio PE, (Italy), BIO in the following). All other reagents were obtained from Sigma–Aldrich (St. Louis, MO, USA).

Samples (Met-ADS and MET-BIO) containing 0.25 g of Met per gram of the carrier were chosen for the experimental trials.

2.1. Sample Preparation and Release Tests

Release tests were performed in water solutions at different pH levels to evaluate the interaction strength between the carrier and Met. The release test procedure is illustrated in Figure 1 and described in detail below. In a typical experiment, 1 g of the carrier (ADS or BIO) was contacted with 50 mL of an aqueous solution at different pH levels, namely 3.0, 5.8, 8.9, by stirring at 600 rpm for 90 min at room temperature. Solid-liquid separation was performed by centrifugation at 3000 rpm for 30 min. The liquid phase, where released Met is expected to be found, was analysed by Chemical Oxygen Demand (COD) [15,16].

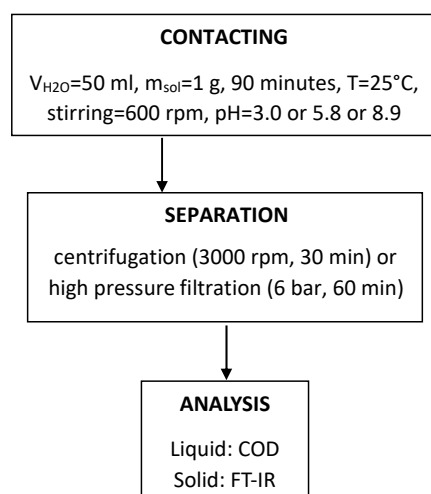


Figure 1. Flow chart of release test procedure.

COD analyses were performed using a Spectrodirect Lovibond Instrument (2021 Tintometer GmbH, www.lovibond.com, accessed on 9 July 2021, Germany) and operated according to standard procedures [ASTM D1252-06]. Aliquots of the liquid phase were stored at $-20\text{ }^{\circ}\text{C}$ for cell viability. Ussing chamber experiments were also performed and are described below.

The residual solid phase was analysed by Fourier Transform Infra-Red (FT-IR) spectroscopy.

FT-IR spectra were recorded in the $4000\text{--}400\text{ cm}^{-1}$ range by a FT-IR Thermo Nicolet Nexus spectrometer (Thermo Electron Corporation, Madison, WI, USA) equipped with a DTGS KBr detector. FT-IR skeletal analyses of inorganic matrix, and other related modified materials were conducted on KBr pressed disks and prepared by carefully mixing the solid sample with KBr powder in an agate mortar (about 1% *w/w* concentration of powders). Measurements were repeated twice with 100 scans each, background air, and in the mid-IR range, i.e., $4000\text{--}400\text{ cm}^{-1}$. FT-IR spectra analysis was performed considering the pH conditions with the lowest recorded release rate.

2.2. Effects of MET-ADS on IPEC-J2 Cell Viability

IPEC-J2 cells are intestinal porcine enterocytes isolated from the jejunum of a neonatal unsuckled piglet (ACC 701, DSMZ, Braunschweig, Germany). The IPEC-J2 cell line is unique as it is derived from the small intestine and is not transformed nor tumorigenic in nature [18]. The IPEC-J2 cells were cultured in DMEM/F-12 mix (Dulbecco's Modified Eagle Medium, Ham's F-12 mixture) supplemented with HEPES, fetal bovine serum (FBS), penicillin/streptomycin and cultivated in a humid chamber at $37\text{ }^{\circ}\text{C}$ with 5% CO_2 . All experiments were performed using IPEC-J2 cells within six cell passages (passages 16 to 22) to ensure reproducibility.

IPEC-J2 cells were seeded at a density of $1.5\text{--}2 \times 10^5$ cells/mL in 96-well plates and cultured for 24 h. In addition, Met-ADS (liquid phase obtained during release tests at pH 3, see above) was tested on IPEC-J2 cell viability. Cell viability was determined after three hours of treatment by a colorimetric proliferation assay (MTT test) in accordance with the manufacturer's instructions (Sigma Aldrich, St. Louis, Missouri, USA).

2.3. Animals and Tissue Collection

The Swiss cantonal Committee for Animal Care and Use approved all procedures involving animals (authorization number: 27428). In total, tissues from $n = 4$ pigs of entire male (EM), Swiss Large White breed were used for the *ex vivo* trial. Only EMs were used to avoid variability related to sex. Pigs were fed a conventional finisher diet and had ad libitum access to drinking water. They were slaughtered at 171 ± 2.8 d of age at the

research station abattoir after being fasted for approximately 15 h. Intestinal segments were removed within 15 min after exsanguination. Intestinal contents were removed with a cold saline solution (4 °C). Tissues were stored in serosal buffer solution (see below) and used for Ussing chamber experiments started within 30 minutes. The jejunum tissues used in the present study were collected from an abattoir for animals entering the food chain; therefore, no ethical issues have been faced. The treatments were performed on tissues mounted in the perfusion chambers and not directly on the animals.

2.4. Ussing Chamber Experiments

For each pig, $n = 6$ jejuna samples starting from the third meter distal to the pylorus were stripped of outer muscle layers and immediately mounted between the two halves of an Ussing chamber (Physiologic Instruments, San Diego, CA, USA). Each segment was bathed on its mucosal and serosal surfaces (exposed area 1.0 cm²) with the same corresponding KRB buffer. Specifically, each chamber was filled with 4 mL KRB buffer (115 mM NaCl, 2.4 mM K₂HPO₄, 0.4 mM KH₂PO₄, 1.2 mM CaCl₂, 1.2 mM MgCl₂, 25 mM NaHCO₃⁻). The serosal buffer (pH 7.4) also contained 10 mM glucose as an energy source that was osmotically balanced by 10 mM mannitol in the mucosal buffer (pH 7.4). Indomethacin was added in both mucosal and serosal buffers (0.01 mM). Buffers were continuously perfused with a 95% O₂ and 5% CO₂ gas mixture. The temperature was maintained at 37 °C by a circulating water bath.

After a stabilization period of 30 min, three different treatments were randomly assigned to each chamber in duplicate: KRB (as control), 2.5 mM pure Met and 2.5 mM of Met-ADS after release tests protocol at pH 3 was applied. The effect of the KRB Buffer pH 3 used for the Met release from the carrier was tested in a different experiment by adding the equivalent volume of the KRB Buffer (pH3) without Met-ADS as a control. Each addition was kept in equilibrated osmotic condition by the addition of equimolar mannitol on the serosal side. Forskolin (10 µM) was added to the serosal compartment at the end of the experiment to test tissue viability. During the experiments, aliquots (500 µL) of both apical and basolateral sides were collected immediately before (T0) and after 3 h (T1) of adding Met. Aliquots were immediately frozen (−20 °C) until further analysis. Trans-epithelial potential difference (TEER) and the short-circuit current (Isc) were continuously monitored using a computer-controlled device. Tissues were voltage-clamped at 0 mV by an external current after correction for solution resistance.

2.5. Quantification of Methionine Release in Luminal and Basolateral Samples

Transepithelial absorption of Met across pig small intestinal mucosa was assessed in apical (mucosal) and basolateral (serosal) aliquots obtained during Ussing chamber experiments (described above) at the beginning of the experiment (0 h) and after the incubation span of 3 h. Samples were thawed rapidly at 20 °C. Quantification of Met was performed by Q-Exactive Orbitrap high-resolution mass spectrometry (HPIEC-HRMS-Orbitrap; Thermo Scientific, San Jose, CA, USA), analysis according to the method described by Panseri et al. [19]. Briefly, after membrane filtration (0.45 µm, PVDF), 3,4,5-trimethoxycinnamic acid (100 mg/L in methanol) was added to an aliquot of 50 µM, and the samples were injected. The temperatures of capillary and vaporizer were set at 330 °C and 280 °C. The electrospray voltage operating in negative mode was adjusted at 3.50 kV.

2.6. Statistical Analysis

Data were analysed using IBM SPSS Statistics version 24 (SPSS, Chicago, IL, USA) and are presented as mean ± standard error. Results were obtained from the minimum of a technical duplicate of four independent experiments. The data were tested for normality using the Shapiro–Wilk test. Results were tested with one-way analysis of variance (ANOVA) as the data were normally distributed. Pairwise comparisons were evaluated using Tukey's HSD test. Differences between control and treatment groups were considered significant when $p < 0.05$.

3. Results

3.1. Release Tests

An exceptionally low amount of Met was found in the liquid phase obtained during the release test. Met-BIO interaction is apparently stronger than Met-ADS. The maximum release of Met was 6% and 3% for Met-ADS and Met-BIO, respectively, at pH 3. Little pH effect can also be inferred considering that, for both solids, the minimum Met released was observed at near-neutral pH, i.e., 5.8 (Table 1).

Table 1. Released methionine at different pH from two different carriers (Adsorbene and BioKi). Tests were performed on 2 g of Met-carrier, which correspond to 0.5 g of total initial methionine in the analysed sample.

Carrier *	pH	Initial Met (g)	Released Met [g]	Release % (<i>w/w</i>)
ADS	3.0	0.50	0.03	6
	5.8		0.01	2
	8.9		0.02	4
BIO	3.0	0.50	0.01	2
	5.8		0.006	1.2
	8.9		0.01	2

* ADS: Adsorbene; BIO: BioKi; Met: Methionine.

Solids after release at pH 5.8, were also analysed by FTIR spectroscopy (Figure 2).

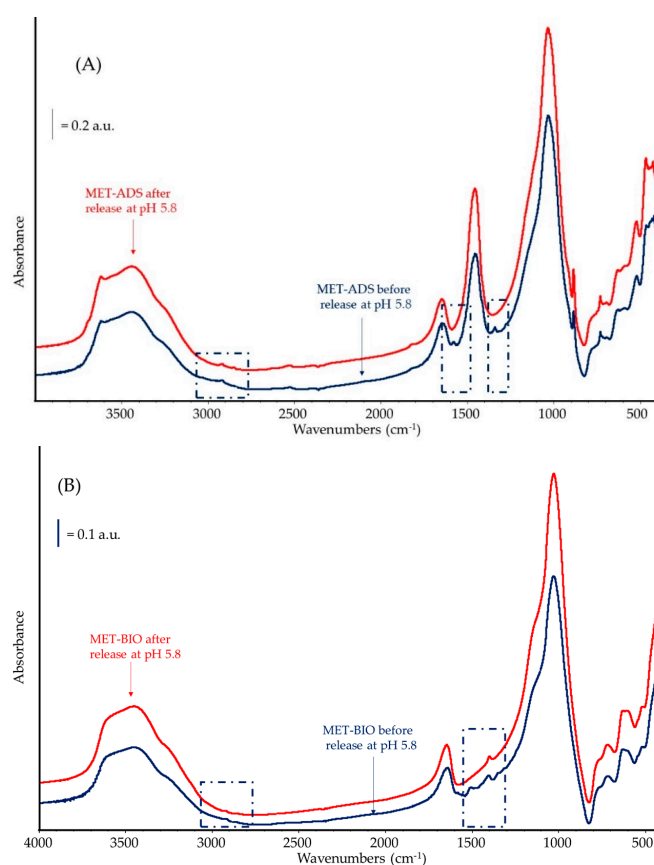


Figure 2. Spectral regions of infrared spectra obtained by Fourier-transform infrared spectroscopy (FTIR) of released methionine at different pH conditions; (A) Met-ADS and (B) Met-BIO before and after release at pH 5.8 (dashed areas: bands of interest). Dashed rectangular: weak IR bands characteristic of the organic moiety near 2920–2950 cm^{-1} (CH stretching modes) and in the region 1620–1300 cm^{-1} (CO and CN stretching modes, CH deformation modes).

In the IR spectrum of both samples before the release test, several weak IR bands characteristic of the organic moiety near $2920\text{--}2950\text{ cm}^{-1}$ (CH stretching modes) and in the region $1620\text{--}1300\text{ cm}^{-1}$ (CO and CN stretching modes, CH deformation modes) are detectable. A detailed spectroscopic investigation on the interaction with methionine and clay matrix has been recently reported by Cristiani et al. (2021, accepted on 14 June). After the release tests, these bands are barely detected in the high-frequency region of the spectrum, namely in the spectrum of the MET-BIO sample (Figure 2B), suggesting the presence of residual Met, strongly bounded at the surface of the carrier.

3.2. Effects of Met-ADS on Intestinal IPEC-J2 Cell Viability

Cell viability experiments revealed that the IPEC-J2 cells treatment with Met-ADS 2.5 mM, and after pre-treatment with KRB, did not significantly altered cell metabolic activity (MTT test) after 3 h contact (Figure 3).

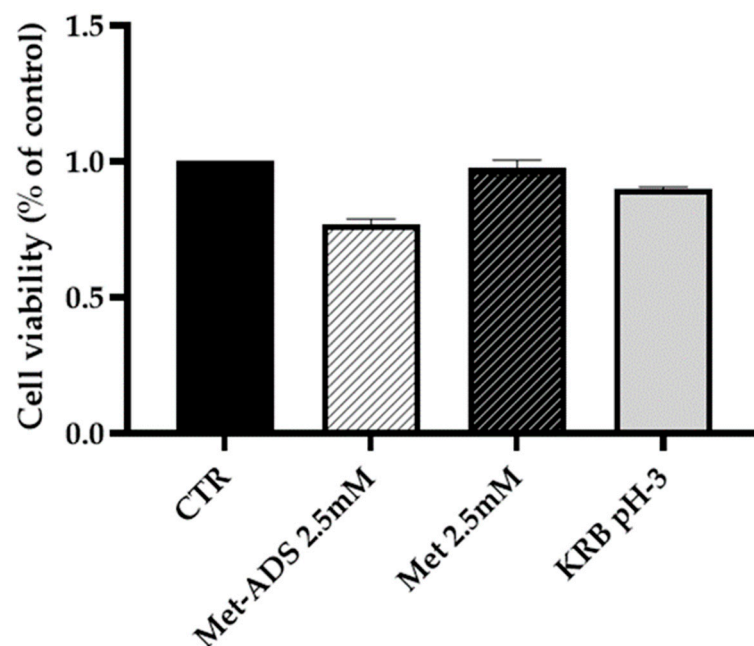


Figure 3. Effect of Met-ADS 2.5 mM and Met 2.5 mM and KRB pH-3 on IPEC-J2 cell viability (percentage of control) after 3 hours incubation.

3.3. Transepithelial Absorption—Ussing Chamber Experiments

The KRB buffer at pH 3 had no effect on the tissue's viability compared to the standard KRB buffer used to carry on the experiments (data not shown).

No differences between Met-ADS and free Met-induced ΔI_{sc} were observed. The high forskolin-induced ΔI_{sc} confirmed the viability of the tissues at the end of the experiment. No detrimental effects on the trans-epithelial resistance were observed in the Met-ADS compared with the controls after 3 h of incubation. Data are reported in Table 2.

Table 2. Induced ΔI_{sc} (μA) and transepithelial resistance (Ω) before (RT0) and 3 h later (RT1) the addition of Kreb's Ringer Buffer (KRB), 2.5 mM free Met and 2.5 mM Met-ADS in pig jejunum. Forskolin-induced ΔI_{sc} ($\Delta I_{sc}\text{-Forsk}$) was evaluated to test tissue viability at the end of the experiment. Data are expressed as mean \pm standard errors.

	KRB	Met 2.5 mM	Met-ADS	<i>p</i> -Values
$\Delta I_{sc}\text{-Met}$	1.96 ± 0.71	3.31 ± 1.0	2.89 ± 0.71	0.37
$\Delta I_{sc}\text{-Forsk}$	25.6 ± 8.48	26.8 ± 10.9	23.4 ± 8.48	0.95
RT0	37.8 ± 3.51	42.1 ± 4.53	36.2 ± 3.51	0.77
RT1	34.8 ± 5.2	43.2 ± 6.67	33.4 ± 5.24	0.69

3.4. Quantification of Methionine in Luminal and Basolateral Samples

The transport of Met occurred across the pig small intestinal mucosa. Results are reported in Table 3. In some cases, Met was not detectable on either the luminal or serosal sides.

Table 3. Methionine percentage investigated in the Ussing chamber with porcine mucosa. Results are presented as a percentage of the luminally applied dose recovered (%) at the beginning of the experiment (0 h) and after 3 h of incubation.

Timepoint	Sample	Sample Condition	Percentage Recovered (%)	
			Luminal	Basolateral
0 h	CTR	KRB buffer pH 7 (no Met)	-	-
	Met-ADS	adsorbene + 25 mM Met pH 3	93.3 ± 5.54	-
	Met 2.5 mM	2.5 mM Met pH 3	108.2 ± 6.76	-
	KRB pH-3	KRB buffer pH 3 (no Met)	-	-
3 h	CTR	KRB buffer pH 7 (no Met)	-	-
	Met-ADS	adsorbene + 25 mM Met pH 3	95.5 ± 8.7	0.72 ± 0.17
	Met 2.5 mM	2.5 mM Met pH 3	107.7 ± 2.7	1.64 ± 0.9
	KRB pH-3	KRB buffer pH 3 (no Met)	-	-

Met = Methionine; ADS = Adsorbene; KRB = Krebs' Ringer Buffer.

As expected, in CTR and KRB pH 3, Met was not detectable in the apical or basolateral compartments of the diffusion chambers at the beginning of the experiment (0 h) or the end (3 h). Contrastingly, in Met-ADS and Met 2.5 mM samples, Met was only detectable on the luminal side at time 0 h. Interestingly, both Met-ADS and Met 2.5 mM reached the basolateral side of the Ussing chamber (0.72 and 1.64%, respectively) after the 3 h trial.

4. Discussion

This study aims to demonstrate the suitability of Met-ADS and Met-Bio as natural AA carriers for animal nutrition application. Given that supplemental dietary AAs need to be provided in a form that prevents their degradation along the gastrointestinal system to guarantee their high bioavailability, bioactivity and absorption, two natural clays are proposed in this study as AAs carrier for feed application. The target of this study is to evaluate possible advantages in the use of clay minerals as carriers of nutrients in feed application. Accordingly, AAs release is a fundamental step that occurs in the intestine of the animal, avoiding the competition for AAs with micro-organisms in the stomach, where absorption by the host is still limited.

The release of Met could result from an external stimulus, such as a change in environmental conditions during the transit of Met through the digestive system. Such stimulus could be the change of pH, which is considered the most important physico-chemical parameter changing in the different parts of the gastrointestinal tract. The ability of pH to affect the release rate of methionine can be exerted on both methionine and carrier; in the case of methionine, by charging the molecule; in the case of the clay, by modifying the interlayer charge. Both these effects may favour methionine release, possibly by charges of repulsion.

4.1. Carriers and Release of Methionine

The synthesis procedure applied to prepare Met-ADS and the Met-BIO samples has demonstrated to be effective in adsorbing the organic molecule onto the carriers. However, considering the different phase composition and structure of the clays, different kinds of

interaction are present in ADS and BIO. In the case of BIO, a pure zeolitic material, MET is trapped inside the zeolitic cages; while in the case of ADS, a mixture of montmorillonite and zeolite-type materials, Met interacts with the carrier via different mechanisms. Indeed, in ADS, the expendable montmorillonitic component can capture Met via both interlayer intercalation, without ions exchange, and surface adsorption, while the zeolitic component behaves as BIO, i.e., via a trapping mechanism (Cristiani et al. 2021, accepted on 14 June).

From the results in Table 1, it is evident that Met is strongly bonded to the carrier. This behavior can be explained considering the nature of the carrier. The ADS is a complex mixture of different mineral clays and zeolites, such as Chabazite (PDF card 01-085-1046), Phillipsite (PDF card 01-072-4634), Bentonite (PDF card 00-003-0015), and Illite (PDF card 01-075-0948). The BIO is a fully zeolite-based material (i.e., Chabazite (PDF card 01-085-1046), Phillipsite (PDF card 01-072-4634), Illite (PDF card 01-075-0948), Hydrosodalite (PDF card 01-073-5304), and Albite (PDF card 19-1184) as found by XRD analysis of the powders. A strong Met trapping by the carrier is present; this is essentially due to the zeolites structural cages, which are able to trap and strongly interact with organic molecules in general. Indeed, the same amount of Met was etched in near- neutral or harsher conditions (i.e., strong acid or base conditions), where a larger release was expected. Therefore, it can be concluded that only Met weakly bounded at the surface of the carrier is released, while no effect of water, high or low pH is exerted on trapped Met.

4.2. Met-ADS and IPEC-J2 Cell Line Viability

Due to the more efficient results obtained by the release tests performed on Met associated with ADS, compared with Bio, only Met-ADS was chosen for the in vitro and ex vivo trials.

Prior studies demonstrated morphological and functional similarities between the IPEC-J2 cell line and intestinal epithelial cells [20]. IPEC-J2 cells mimic the intestinal physiology more closely than any other cell line of tumor origin. Therefore, they are ideal tools to study epithelial transport and the effect of nutrients on a variety of parameters reflecting epithelial functionality [18,21,22].

In this study, IPEC-J2 cells were used as an in vitro model to study the effects of Met-ADS in order to exclude any cytotoxicity issue at the intestinal epithelium level before ex vivo trials. Results from IPEC-J2 experiments did not reveal statistically significant toxicity in IPEC-J2 cells treated with Met-ADS, suggesting that Adsorbene did not cause detrimental effects on the intestinal epithelial tissue after 3 h of contact [23]. Once the safety of the Met-ADS products on intestinal epithelial cells was assumed, the absorption of the Met released by the ADS was tested in porcine explants *ex vivo*.

4.3. Methionine Absorption in Pig Jejunum

In the present study, we tested the absorption of Met released from Met-ADS complex in porcine jejunum *ex vivo*. Exogenous Met is commonly added to diets that do not contain a sufficient amount of Met to meet the Met requirement by the pig. To be transported from the intestinal lumen into the blood, Met enter the intestinal absorptive epithelial cells (a.k.a. enterocytes) first through corresponding transporters present in the brush border membrane at the apical side and then exported from the epithelial cells to the bloodstream through the transporters present in the basolateral membrane [24]. Met is a neutral AA, and its uptake across the apical membrane of intestinal epithelial cells is almost entirely Na⁺-dependent [25,26]. The major apical neutral AA transporter in the intestine is the B(0)AT1 (SLC6A19) system, which cotransports one Na⁺ per AA [27]. In pigs, Met is absorbed along the entire small intestinal tract.

The Ussing system offers an *ex vivo* measurement of electrophysiological measurements such as TEER (as a measurement of gut integrity) and short circuit current (I_{sc}). I_{sc} is a summation of all ionic currents across the epithelium, and it represents an estimation of actively transported ions across the epithelial membrane [17]. However, once absorbed, Met can be metabolised by the epithelial cells or released in the serosal side of the epithe-

lium. In order to estimate the quantity of Met released in the serosal side, Ussing-obtained data must be integrated with other techniques such as Mass Spectroscopy.

In this study, we used jejunum segments because previous studies in pigs demonstrated that the rate of Met absorption in this region is comparable with or exceeds those of other regions [28]. During the 3 h exposure time of the jejunum segments, a small percentage of both free Met and Met-ADS were absorbed. The low percentage of both Met and Met-ADS absorbed during the trial could be explained by the saturable absorption of the Met. Concentrations tested in our study were chosen to ensure the saturation of the intestinal carriers. The maximum rates of saturable absorption of Met has been estimated in the range of $\text{nmol min}^{-1} \text{mg tissue}^{-1}$ by the middle intestine [28]. However, the lack of statistically significant difference in the Met and Met-ADS-induced ΔIsc demonstrated that ADS did not affect the potential of the Met to be absorbed by the intestinal active transporters once released by the carrier. In agreement with the cytotoxicity test in vitro, no detrimental effects on the intestinal epithelial integrity were observed. Specifically, no differences in the TEER between CTR, Met and Met-ADS were found. In all the groups, the TEER remained nearly constant during the whole experiment demonstrating that the integrity lasted for the entire trial. The forskolin-induced ΔIsc values also confirmed the viability of the tissues at the end of the experiment, confirming the absence of detrimental effects of Met-ADS on jejunum integrity.

5. Conclusions

This study offers new insights into the release of Met from ADS and BIO, the safety of its use in the porcine intestine and the ability of ADS-released Met to be absorbed to the same extent as the free Met in porcine jejunum. Although the application of delivery systems may represent an efficient solution for reducing peptide-food matrix reactions and improving amino acid bioavailability in swine feed, further studies need to focus on optimising delivery systems to maximise amino acid release at relevant gastrointestinal conditions.

Author Contributions: Conceptualization, C.G., M.T., C.C. and L.R.; methodology, C.G., M.T., C.C. and E.F.; formal analysis, C.G., M.T., C.C., E.F., and S.P.; investigation, C.G., M.T., C.C., E.F., P.S. and S.P.; resources, C.C. and L.R.; data curation, C.G., M.T. and C.C.; writing—original draft preparation, C.G., M.T., C.C. and E.F.; writing—review and editing, C.G., M.T., C.C., E.F., P.S., S.P. and M.D.; visualization, C.G., C.C. and E.F.; supervision, A.B.; project administration, L.R.; funding acquisition, L.R. All authors have read and agreed to the published version of the manuscript.

Funding: This research was funded by the Lombardy Region and European Regional Development Fund (ERDF) under grant: FoodTech Project (ID: 203370).

Institutional Review Board Statement: The study was conducted according to the guidelines of the Declaration of Helsinki.

Informed Consent Statement: Not applicable.

Data Availability Statement: The data presented in this study are available within the article.

Acknowledgments: We are grateful to ProPhos Chemicals S.r.l. for project coordination.

Conflicts of Interest: The authors declare no conflict of interest.

References

1. Rossi, L.; Dell'Orto, V.; Vagni, S.; Sala, V.; Reggi, S.; Baldi, A. Protective effect of oral administration of transgenic tobacco seeds against verocytotoxic *Escherichia coli* strain in piglets. *Vet. Res. Commun.* **2014**, *38*, 39–49. [[CrossRef](#)] [[PubMed](#)]
2. Rossi, L.; Di Giancamillo, A.; Reggi, S.; Domeneghini, C.; Baldi, A.; Sala, V.; Dell'Orto, V.; Coddens, A.; Cox, E.; Fogher, C. Expression of verocytotoxic *Escherichia coli* antigens in tobacco seeds and evaluation of gut immunity after oral administration in mouse model. *J. Vet. Sci.* **2013**, *14*, 263–270. [[CrossRef](#)] [[PubMed](#)]
3. Rossi, L.; Pinotti, L.; Agazzi, A.; Dell'Orto, V.; Baldi, A. Plant bioreactors for the antigenic hook-associated flgK protein expression. *Ital. J. Anim. Sci.* **2014**, *13*, 2939. [[CrossRef](#)]

4. Wang, Y.; Zhou, J.; Wang, G.; Cai, S.; Zeng, X.; Qiao, S. Advances in low-protein diets for swine. *J. Anim. Sci. Biotechnol.* **2018**, *9*, 1–14. [[CrossRef](#)] [[PubMed](#)]
5. Yang, Z.; Htoo, J.K.; Liao, S.F. Methionine nutrition in swine and related monogastric animals: Beyond protein biosynthesis. *Anim. Feed Sci. Technol.* **2020**, *268*, 114608. [[CrossRef](#)]
6. Zimmermann, B.; Mosenthin, R.; Rademacher, M.; Lynch, P.; Esteve-Garcia, E. Comparative studies on the relative efficacy of DL-methionine and liquid methionine hydroxy analogue in growing pigs. *Asian-Australas. J. Anim. Sci.* **2005**, *18*, 1003–1010. [[CrossRef](#)]
7. Kim, B.; Lindemann, M.; Rademacher, M.; Brennan, J.; Cromwell, G. Efficacy of DL-methionine hydroxy analog free acid and DL-methionine as methionine sources for pigs. *J. Anim. Sci.* **2006**, *84*, 104–111. [[CrossRef](#)]
8. Wen, C.; Chen, X.; Chen, G.; Wu, P.; Chen, Y.; Zhou, Y.; Wang, T. Methionine improves breast muscle growth and alters myogenic gene expression in broilers. *J. Anim. Sci.* **2014**, *92*, 1068–1073. [[CrossRef](#)]
9. Kong, C.; Ahn, J.Y.; Kim, B.G. Bioavailability of D-methionine relative to L-methionine for nursery pigs using the slope-ratio assay. *PeerJ* **2016**, *4*, e2368. [[CrossRef](#)]
10. Zaninelli, M.; Rossi, L.; Tangorra, F.M.; Costa, A.; Agazzi, A.; Savoini, G. On-line monitoring of milk electrical conductivity by fuzzy logic technology to characterise health status in dairy goats. *Ital. J. Anim. Sci.* **2014**, *13*, 3170. [[CrossRef](#)]
11. Toledo, M.Z.; Stangaferro, M.L.; Gennari, R.S.; Barletta, R.V.; Perez, M.M.; Wijma, R.; Sitko, E.M.; Granados, G.; Masello, M.; Van Amburgh, M.E.; et al. Effects of feeding rumen-protected methionine pre- and postpartum in multiparous Holstein cows: Lactation performance and plasma amino acid concentrations. *J. Dairy Sci.* **2021**, *104*, 7583–7603. [[CrossRef](#)]
12. Amigo, L.; Hernández-Ledesma, B. Current evidence on the bioavailability of food bioactive peptides. *Molecules* **2020**, *25*, 4479. [[CrossRef](#)]
13. Sun, X.; Acquah, C.; Aluko, R.E.; Udenigwe, C.C. Considering food matrix and gastrointestinal effects in enhancing bioactive peptide absorption and bioavailability. *J. Funct. Foods* **2020**, *64*, 103680. [[CrossRef](#)]
14. McClements, D.J. Advances in nanoparticle and microparticle delivery systems for increasing the dispersibility, stability, and bioactivity of phytochemicals. *Biotechnol. Adv.* **2020**, *38*, 107287. [[CrossRef](#)] [[PubMed](#)]
15. Cristiani, C.; Iannicelli-Zubiani, E.M.; Bellotto, M.; Dotelli, G.; Stampino, P.G.; Latorrata, S.; Ramis, G.; Finocchio, E. Capture Mechanism of La and Cu ions in mixed solutions by clay and organoclay. *Ind. Eng. Chem. Res.* **2021**, *60*, 6803–6813. [[CrossRef](#)]
16. Cristiani, C.; Iannicelli-Zubiani, E.M.; Bellotto, M.; Dotelli, G.; Finocchio, E.; Latorrata, S.; Ramis, G.; Stampino, P.G. Capture and release mechanism of La ions by new polyamine-based organoclays: A model system for rare-earths recovery in urban mining process. *J. Environ. Chem. Eng.* **2021**, *9*, 104730. [[CrossRef](#)]
17. Thomson, A.; Smart, K.; Somerville, M.S.; Lauder, S.N.; Appanna, G.; Horwood, J.; Raj, L.S.; Srivastava, B.; Durai, D.; Scurr, M.J. The Ussing chamber system for measuring intestinal permeability in health and disease. *BMC Gastroenterol.* **2019**, *19*, 98. [[CrossRef](#)]
18. Vergauwen, H. The IPEC-J2 cell line. In *Impact of Food Bioactives on Health*; Springer: Cham, Switzerland, 2015; pp. 125–134.
19. Panseri, S.; Arioli, F.; Biolatti, C.; Mosconi, G.; Pavlovic, R.; Chiesa, L.M. Detection of polyphosphates in seafood and its relevance toward food safety. *Food Chem.* **2020**, *332*, 127397. [[CrossRef](#)]
20. Schierack, P.; Nordhoff, M.; Pollmann, M.; Weyrauch, K.D.; Amasheh, S.; Lodemann, U.; Jores, J.; Tachu, B.; Kleta, S.; Blik-slager, A.; et al. Characterization of a porcine intestinal epithelial cell line for in vitro studies of microbial pathogenesis in swine. *Histochem. Cell Biol.* **2006**, *125*, 293–305. [[CrossRef](#)]
21. Reggi, S.; Giromini, C.; Dell'Anno, M.; Baldi, A.; Rebutti, R.; Rossi, L. In vitro digestion of chestnut and quebracho tannin extracts: Antimicrobial effect, antioxidant capacity and cytomodulatory activity in swine intestinal IPEC-J2 cells. *Animals* **2020**, *10*, 195. [[CrossRef](#)]
22. Sundaram, T.S.; Giromini, C.; Rebutti, R.; Baldi, A. Omega-3 polyunsaturated fatty acids counteract inflammatory and oxidative damage of non-transformed porcine enterocytes. *Animals* **2020**, *10*, 956. [[CrossRef](#)]
23. Davis, S.; Illum, L.; Hinchcliffe, M. Gastrointestinal transit of dosage forms in the pig. *J. Pharm. Pharmacol.* **2001**, *53*, 33–39. [[CrossRef](#)] [[PubMed](#)]
24. Matthews, J. Amino acid and peptide transport systems. In *Farm Animal Metabolism and Nutrition*; CABI: Wallingford, UK, 2000; pp. 3–23.
25. Bröer, S. Amino acid transport across mammalian intestinal and renal epithelia. *Physiol. Rev.* **2008**. [[CrossRef](#)] [[PubMed](#)]
26. Romanet, S.; Aschenbach, J.R.; Pieper, R.; Zentek, J.; Htoo, J.K.; Whelan, R.A.; Mastrototaro, L. Dietary supplementation of dl-methionine potently induces sodium-dependent l-methionine absorption in porcine jejunum *ex vivo*. *J. Nutr.* **2020**, *150*, 1782–1789. [[CrossRef](#)] [[PubMed](#)]
27. Camargo, S.M.; Makrides, V.; Virkki, L.V.; Forster, I.C.; Verrey, F. Steady-state kinetic characterization of the mouse B 0 AT1 sodium-dependent neutral amino acid transporter. *Pflügers Arch.* **2005**, *451*, 338–348. [[CrossRef](#)] [[PubMed](#)]
28. Buddington, R.K.; Elnif, J.; Puchal-Gardiner, A.A.; Sangild, P.T. Intestinal apical amino acid absorption during development of the pig. *Am. J. Physiol. Regul. Integr. Comp. Physiol.* **2001**, *280*, R241–R247. [[CrossRef](#)] [[PubMed](#)]